

Hyperbox modeling of CFRP shear contribution on retrofitted RC structures

*Alvin Chua¹, Kathleen Aviso², and Jason Maximino Ongpeng³

^{1,3} *Department of Civil Engineering, DLSU, Manila, Philippines*

² *Department of Chemical Engineering, DLSU, Manila, Philippines*

¹ alvin_chua@dlsu.edu.ph

ABSTRACT

The shear mechanics of externally bonded (EB) CFRP on beams is a complex issue that is not yet fully understood because of their several possible failure modes. Uncontrolled responses in the composite RC system is attributable to EB CFRPs having lesser anchorage on the concrete. Many studies and real-life applications have used machine learning (ML) techniques to solve complex problems using datasets. Hyperbox modeling is an ML approach that provides interpretability and versatility in results generation. This study presents models using hyperboxes to determine if the shear strength contribution of the carbon fiber reinforced polymer (CFRP) on the reinforced concrete (RC) beams is sufficient. A novel feature of the approach is the ability to minimize misclassification errors (e.g., false positives) during the algorithm's training phase. The produced models were then compared with existing design codes to assess their performance, resulting in an accuracy yield of about 80%. Overall, this study shows that ML-derived rule-based decision models can sufficiently serve as a quick analysis guide in areas where certain behaviors or mechanics (like shear) have not yet been fully understood.

1. INTRODUCTION

Concrete structures inevitably undergo degradation. The speed and severity of the degradation depend on numerous factors (e.g., temperature, hazards encountered). Retrofitting is a rehabilitative measure undertaken to mitigate the effects of such degradation, if not fully restore or enhance the original strength of the RC structure (Shrikande 2006). CFRPs are an example of retrofitting materials often used in civil engineering applications. Their versatility, strength, non-intrusiveness, and lightweight properties have been attributed to their frequent utilization and focus in research (Pampanin et al 2007; Das 2011).

¹ Graduate Student, M.Sc.

² Professor, Ph.D.

³ Professor, D. Eng.

*The 2022 World Congress on
The 2022 Structures Congress (Structures22)
16-19, August, 2022, GECE, Seoul, Korea*

The CFRPs allow for multiple ways of strengthening (e.g., flexure, axial, and shear) RC structures in civil engineering applications (Colotti 2016). Among the many strengthening applications in structural mechanics, shear behavior is often regarded as the most difficult, having the most internal interactions that are not yet fully understood (Schmidt et al 2021). Researchers have developed numerous models to capture each component's interaction and respective contributions to shear-strengthened RC members (e.g., stirrups and concrete). This complexity is why shear equations in design codes are generally empirical, contrary to the theoretical nature of flexural and axial equations. The complexity of shear behavior in shear-strengthened RC members is enhanced when considering the applications of composite materials like CFRPs. The considerations in equations covering composite materials include (a) flexural-shear interaction failure modes, including the contribution of external shear reinforcement; (b) shear web-crushing; and (c) pure flexural failure modes (Abuodeh et al 2020).

Retrofitting shear-deficient RC beams commonly practice two external bonding (EB) configurations. These are the side-bonded and U-wrapped configurations. Complete wrapping of CFRPs on beams can achieve similar, if not better, results; however, the side-bonded and U-wrapped compositions are preferred in terms of practicality and ease of application (Colotti 2016). These setups, however, subject the composite RC system to failure modes like CFRP debonding and rupture. Analytical and experimental studies were conducted to understand the shear contribution of EB CFRP on retrofitted shear-deficient RC beams. The models produced reveal that a parameter called effective strain (alternatively called effective stress) is commonly used (Oller et al 2021; Zhou et al 2020; Chen et al 2013). A governing failure mode (e.g., debonding) often limits this parameter. Unfortunately, due to the many complicated, interrelated factors and mechanisms mentioned earlier, there has yet to be a consensus on how this parameter should be derived. Ultimately, the numerous unknown parameters and interactions in the CFRP-RC system often led to unoptimized use of the material and over-conservative assumed values in designing (Pohoyryles 2016). The inability to safely predict shear-related failure is critical (relative to flexural failure) because of the brittle mode of failure associated. Such failure implies that a warning (e.g., cracks) indicating impending failure will not be given or easily seen.

The civil engineering field faces a lot of complicated problems in various facets. Researchers have utilized tools like ML to tackle complex issues. Unlike more popular branches of ML, like the artificial neural networks (ANNs), the hyperbox membership classification is a technique that has not yet become mainstream (Tan et al 2020). A significant disadvantage of ANNs is that it is subject to "catastrophic forgetting," making the model unable to retain previously learned patterns when new patterns become available (Chaabene et al 2020). This issue is more significant when the primary users are not the researchers themselves.

On the other hand, hyperbox classification is a versatile tool that can provide quickly interpretable rules when decision support is required. They provide distinct advantages like nonlinear separability, overlapping region, invulnerability, provision of soft and hard decisions, shortened training time, verification and validation, and

*The 2022 World Congress on
The 2022 Structures Congress (Structures22)
16-19, August, 2022, GECE, Seoul, Korea*

parameter adjustment minimization (Xu and Papageorgiou 2009). Three categories of the learning model have been identified thus far: neural network structured, non-network structured, and hybrid tree and network structured (Khuat et al 2020). The neural network structured approach is the most common model and is further categorized into two learning groups. The fuzzy min-max neural network (FMMNN) is the most famous model within this category. It cannot, however, yield a compact rule set because many hyperboxes can be generated (Alhroob et al 2019). Alternatively, a non-network structured approach like the mixed integer linear programming (MILP) model can limit the number of hyperboxes generated. This approach enables the production of a compacted and optimized rule set, minimizing the number of misclassifications by finding the optimal hyperbox dimension and positions (Xu and Papageorgiou 2009).

The hyperbox categorization model, through the IF-THEN formatting of the generated rules, alleviates the interpretability issue that some ML models face. Aviso et al (2021) presented a novel MILP framework for hyperbox classification modeling. It features the ability to optimize the generated model by explicitly accounting for the Type 1 (false positive) and Type 2 (false negative) errors. Contrary to other ML models that rely on statistical parameters (e.g., RMSE), the hyperbox modeling approach relies on classification validation results. This feature enables the adequate prediction of CFRP shear strength contribution sufficiency (i.e., safe or unsafe) considering the complex mechanics and the unfinished determination of some essential parameters (e.g., effective stress). The classification model used in this study also adopts a holistic overview that does not disregard any shear action (both known and unknown).

The subsequent chapters of this paper tackle the research methodology (Section 2), the machine learning model framework (Section 3), results and discussion (Section 4), and the conclusions and recommendations (Section 5). Section 2 describes the development of the database and illustrates a brief overview of the experimental characteristics considered. The most influential parameters, as determined by the fitted decision tree algorithm, are likewise presented. Section 3 demonstrates the algorithm variables and equations used to produce the hyperboxes. Section 4 shows the models produced by the hyperbox ML and the corresponding performances through confusion matrices and design code comparatives. The confusion matrices summarize the prediction performances of the ML algorithm. Finally, Section 6 presents the concluding remarks.

2. RESEARCH METHODOLOGY

The formulation of the rule-based models using the hyperbox classification model requires a database of sufficient size. Hence, this study initially analyzed 589 experimental simply supported beam specimens from 65 studies, covering the period of 1997 to 2020. The most featured articles in the database were from Elsevier (25 studies), ASCE (17 studies), and ACI (8 studies). Overall, through the number of CFRP retrofitted RC beams, the database addresses the issues found in other analytical studies, such as (1) insufficient experimental RC beams to represent other specimens;

*The 2022 World Congress on
The 2022 Structures Congress (Structures22)
16-19, August, 2022, GECE, Seoul, Korea*

(2) no emphasis on FRP configuration; (3) no consideration for the anchorage effect of some CFRP configurations. It should be noted that only simply supported beams strengthened in shear with rectangular or T-shaped cross sections were investigated. Moreover, beams with any anchorage effect were excluded from this study. An overview of the initially considered parameters is as follows:

- **Beam geometry** – beam height, width, span length, section (rectangular or T-shaped), and effective depth
- **Concrete compressive strength**
- **Loading** – span-to-depth ratio, three- or four-point loading
- **Steel characteristics** – type (plain or deformed), diameter, reinforcement ratio, yield strength, ultimate strength, and modulus of elasticity
- **FRP characteristics** – number of layers, thickness, tensile strength, reinforcement ratio, modulus of elasticity, type (unidirectional or bidirectional), kind (side strip, side continuous sheet, U-strip, U-continuous sheet), angle, FRP width, FRP spacing, effective FRP depth, and ultimate strain
- **Experimental failure load**

The initial number of parameters was reduced for the eventual processing of the parameter selection algorithm. The parameters that were consistently available across most, if not all, studies and had little to no need for assumptions were considered for further processing under the algorithm. External experimental factors (e.g., humidity) that were seen only in some studies were not taken for further processing. The compiled data samples underwent a min-max normalization to eliminate irrelevant and anomalous data. The normalization follows the equation below:

$$v' = \frac{v - \min_A}{\max_A - \min_A} (\max_{A,new} - \min_{A,new}) + \min_{A,new} \quad (1)$$

where:

v'	output value in the specified range
v	input value in the original range
\max_A	maximum value in the original range
\min_A	minimum value in the original range
$\max_{A,new}$	maximum value in the specified range
$\min_{A,new}$	minimum value in the specified range

Efficient algorithm analysis in determining the most influential parameters is essential to yielding accurate rule-based decision models using the hyperbox tool. A fitted decision tree algorithm using MATLAB was executed for this purpose. Decision trees are among the most utilized methods in data mining for their versatility, interpretability, and conciseness. The algorithm processing revealed that there are

*The 2022 World Congress on
The 2022 Structures Congress (Structures22)
16-19, August, 2022, GECE, Seoul, Korea*

seven influential parameters affecting V_f . These parameters are elaborated, in order of influence, with basic statistical features in Table 1.

Table 1. Basic statistical information on the influential determined parameters.

Parameter	Symbol	Min.	Max.	Mean	Std. Dev.
Concrete compressive strength	f'_c , MPa	12.4	71.4	36.7	12.6
Shear span-to-depth ratio	a/d	1.19	6.90	2.77	0.73
Stirrup reinforcement ratio	ρ_s	0.000	0.010	0.003	0.002
Longitudinal reinforcement ratio	ρ_L	0.005	0.075	0.023	0.011
FRP reinforcement ratio	ρ_{FRP}	0.0002	0.0889	0.0048	0.0075
Effective FRP depth	d_f , mm	50.0	762.0	292.3	120.1
Ultimate FRP strain	ε_{u_s} , %	4.0	21.3	15.1	3.4

A criterion must first be established to determine if the retrofitted CFRP-RC composite system can be considered safe. The designation of “safe” is given to retrofitted RC beams with sufficient CFRP shear strength contribution (V_f). As seen in other studies (Naderpour & Alavi 2017; Ma et al 2019; Zhou et al 2020; Oller et al 2021), the safety remark is set through the parameter μ (“mu”), with values greater than one (1) regarded as safe. The following equation defines this criterion:

$$\mu = V_{f,experimental}/V_{f,theoretical} \quad (2)$$

The values for $V_{f,experimental}$ refer to the ultimate shear strength of the RC beams retrofitted with EB CFRPs. Many models predicting V_f have been formulated through experimental or analytical means. It can be observed from many studies that a common source of variation among the prediction models is the parameter effective strain, ε_{fe} , or its alternate form, effective stress, f_{fe} (Chen et al 2013; Abuodeh et al 2020; Kar et al 2021). This variability can be attributed to the various means of derivation, assumptions, and methods in determining the effective strain. A single equation for $V_{f,theoretical}$ must thus be chosen. Hence, this study considers the model provided by the design code *fib 14* as the basis for $V_{f,theoretical}$. The values for $V_{f,theoretical}$ will be used to determine the associated μ values for each sample to be processed by the ML program. The corresponding μ values are essential to optimizing the dimensions and positions of the hyperboxes, as shown in the succeeding chapter. Considering limitations of the ML framework, the study only processed the samples that followed the given range of $[0.7 \leq \mu \leq 1.3]$. Large spreads for μ made the program unable to reach a global optimum. The range restriction reduced the number of training samples to only 76 beams. Nevertheless, the study managed to produce sufficiently accurate models.

The 2022 World Congress on
The 2022 Structures Congress (Structures22)
 16-19, August, 2022, GECE, Seoul, Korea

3. MACHINE LEARNING FRAMEWORK

The rule-based decision equations produced from the hyperbox classification algorithm follow a novel MILP framework, as seen in [Tan et al. \(2020\)](#). The IF/THEN binary approach to misclassifications can be altered depending on the critical scenario (i.e., minimize false positives or negatives). This capability enables the optimization of the iterative binary rule generation. The algorithm variables are given as follows:

Indices:

- j sample ($j = j_1, j_2, \dots, J$)
- i attribute ($i = i_1, i_2, \dots, i_7$)
- k hyperbox that sample j belongs to

Sets:

- S^N all negative values used for training
- S^P all positive values used for training
- N^T total number of samples in S^N
- P^T total number of samples in S^P

Parameters:

- X_{ji} value of sample j for attribute i
- x_{ik}^L lower bound of hyperbox k in dimension i
- x_{ik}^U upper bound of hyperbox k in dimension i
- Z_{ik}^L lowest possible value of dimension i in hyperbox k
- Z_{ik}^U highest possible value of dimension i in hyperbox k
- ϵ misclassification probability threshold
- M arbitrary large number for hyperbox generation

Binary Variables:

- c_j 1 if predicted V_f is safe, else 0
- C_j^* 1 if actual V_f is safe, else 0
- b_{ik}^L inner lower hyperbox boundary activator
- b_{ik}^U inner upper hyperbox boundary activator
- q_{ik}^L outer lower hyperbox boundary activator
- q_{ik}^U outer upper hyperbox boundary activator

Misclassification Variables:

- ω false positive
- γ false negative

The 2022 World Congress on
The 2022 Structures Congress (Structures22)
 16-19, August, 2022, GECE, Seoul, Korea

Determining the dimensions of each hyperbox is essential to classifying the samples for the bi-objective MILP. Each sample j is assigned a corresponding performance attribute i . The iterative binary rule generation minimizing the false positives in the dataset ran as follows. Eq. (4) and (5) define the proportions for the false positives and false negatives, respectively. Eq. (6) represents the threshold for the false negatives.

$$\min \omega \quad (3)$$

$$\omega = \frac{\sum_j (c_j - C_j^*)}{N^T}, \quad \forall j \in S^N \quad (4)$$

$$\gamma = \frac{\sum_j (C_j^* - c_j)}{P^T}, \quad \forall j \in S^P \quad (5)$$

$$\gamma \leq \varepsilon \quad (6)$$

The outer and inner boundaries of the hyperboxes are defined by Eq. (7)-(8) and (9)-(10), respectively. The binary output variable, b_{jk} , is given a value of 1 if the sample is within the hyperbox; otherwise, a value of 0 is assigned. The lower (x_{ik}^L) and upper (x_{ik}^U) boundaries are defined by Eq. (11)-(12) and (13)-(14), respectively.

$$X_{ji} > x_{ik}^L - \Delta - M(1 - b_{jk}), \quad \forall i, j \quad (7)$$

$$X_{ji} < x_{ik}^L + \Delta + M(1 - b_{jk}), \quad \forall i, j \quad (8)$$

$$X_{ji} > x_{ik}^L - M(1 - b_{jk}), \quad \forall i, j \quad (9)$$

$$X_{ji} < x_{ik}^L + M(1 - b_{jk}), \quad \forall i, j \quad (10)$$

$$Z_{ik}^L - M(1 - b_{ik}^L) \leq x_{ik}^L \leq Z_{ik}^L + Mb_{ik}^L, \quad \forall i, k \quad (11)$$

The 2022 World Congress on
The 2022 Structures Congress (Structures22)
 16-19, August, 2022, GECE, Seoul, Korea

$$\begin{cases} Z_{ik}^L \leq x_{ik}^L \leq Z_{ik}^L + M & \forall i, k, & b = 1 \\ Z_{ik}^L - M \leq x_{ik}^L \leq Z_{ik}^L & \forall i, k, & b = 0 \end{cases} \quad (12)$$

$$Z_{ik}^U - Mb_{ik}^U \leq x_{ik}^U \leq Z_{ik}^U + M(1 - b_{ik}^U), \quad \forall i, k \quad (13)$$

$$\begin{cases} Z_{ik}^U - M \leq x_{ik}^U \leq Z_{ik}^U & \forall i, k, & b_{ik}^U = 1 \\ Z_{ik}^U \leq x_{ik}^U \leq Z_{ik}^U + M & \forall i, k, & b_{ik}^U = 0 \end{cases} \quad (14)$$

Eq. (15)-(16) determines if a given sample j is within the dimensions of a given attribute i . The binary output variable is given a value of 0 if the sample lies outside the hyperbox. This scenario assigns a value of 1 to the outer activation variables (q_{ik}^L and q_{ik}^U), as defined by Eq. (17) and (18). If the sample is within any of the produced hyperbox dimensions, Eq. (19) designates a value of 1 to the variable c_j . Eq. (20) is used to contract the hyperbox dimensions. Eq. (21) is a constraint for all binary variables used in the algorithm.

$$X_{ji} \leq x_{ik}^L - \Delta + M(1 - q_{ijk}^L), \quad \forall i, j \quad (15)$$

$$X_{ji} \geq x_{ik}^U + \Delta - M(1 - q_{ijk}^U), \quad \forall i, j \quad (16)$$

$$\sum_i q_{ijk}^L + q_{ijk}^U \leq M(1 - b_{jk}), \quad \forall j, k \quad (17)$$

$$\sum_i q_{ijk}^L + q_{ijk}^U \geq (1 - b_{jk}), \quad \forall j, k \quad (18)$$

$$\sum_k b_{jk} \leq Mc_j, \quad \forall j \quad (19)$$

$$\sum_k b_{jk} \geq c_j, \quad \forall j \quad (20)$$

$$b_{jk}, b_{ik}^U, b_{ik}^L, Q_{ijk}^U, Q_{ijk}^L, C_j \in \{0,1\} \quad (21)$$

4. RESULTS AND DISCUSSION

The hyperbox classification algorithm using the novel MILP framework of [Tan et al. \(2020\)](#) generated rule-based decision models for the CFRP retrofitted RC beams. During the data processing, the dataset was divided into two groups: training (60%) and validation (40%). Each training setup gave results for the two CFRP configurations under investigation (i.e., side-bond and U-wrap). The format of the rule-based decision models (representing one hyperbox each) which determines safe composite systems are as follows:

$$\text{IF } x_1^L \leq i_1 \leq x_1^U \text{ AND } x_2^L \leq i_2 \leq x_2^U \dots \text{ AND } x_N^L \leq i_N \leq x_N^U \text{ THEN } V_f = 1$$

False positives and negatives have critical implications for both the composite systems and the model predictions. Thus, their corresponding rough translations are given below. Type 1 errors, or false positives, pose severe threats in structural retrofitting considering the brittle nature of shear failure; hence, it is treated as the critical misclassification error in this study.

Type 1 error (false positive): The beam is identified as adequately strengthened in shear by the EB CFRP, but it is actually not sufficiently strengthened.

Type 2 error (false negative): The beam is identified as inadequately strengthened in shear by the EB CFRP, but it is actually sufficiently strengthened.

The first set of rules was generated to minimize the false negatives (γ) while keeping the false positives (ω) less than 0. The summary of the lower and upper bounds for the side-bonded and U-wrapped CFRP is shown in Table 2.

Table 2. Boundaries for the parameters under Rule 1.

Parameter	Unit	Side-bonded		U-wrapped	
		X_i^L	X_i^U	X_i^L	X_i^U
f_c'	MPa	22.2	61.0	24.9	35.0
a/d	-	1.19	3.20	1.50	5.02
ρ_s	-	-	0.003	-	0.008
ρ_L	-	0.012	0.040	0.021	0.048
ρ_{FRP}	-	0.0010	0.0222	0.0007	0.0019
d_f	mm	107.5	417.1	285.0	482.6
ε_u	%	7.7	19.2	10.4	20.7

The results for Rule 1 indicate that the rule applies to all retrofitted beams regardless of the internal transverse reinforcements. After the dimensions have been obtained through the training phase, the model will undergo the validation phase. The

*The 2022 World Congress on
The 2022 Structures Congress (Structures22)
16-19, August, 2022, GECE, Seoul, Korea*

prediction performances of the models for the validation phase, through the dimensions of “actual” and “predicted”, are shown in confusion matrices. Results show that 13 of 13 safe retrofitted beams and 4 of 13 unsafe retrofitted beams were correctly identified, as summarized in the following confusion matrices (Table 3 and Table 4). Sample calculations to determine the false positives (ω_V) and false negatives (γ_V) are given as follows. These calculations are valid for all succeeding confusion matrix calculations.

Type 1 errors / false positives of the validation group (ω_V) for Rule 1 (side-bonded):

$$\omega_V = \frac{4 - 4}{4} = 0.000$$

Type 2 errors / false negatives of the validation group (γ_V) for Rule 1 (side-bonded):

$$\gamma_V = \frac{22 - 13}{22} = 0.409$$

Type 1 errors / false positives of the validation group (ω_V) for Rule 1 (U-wrapped):

$$\omega_V = \frac{15 - 14}{15} = 0.067$$

Type 2 errors / false negatives of the validation group (γ_V) for Rule 1 (U-wrapped):

$$\gamma_V = \frac{7 - 1}{7} = 0.857$$

Table 3. Confusion matrix for side-bond CFRP using Rule 1 ($\omega_V = 0.000$; $\gamma_V = 0.409$).

N = 26	Actual safe	Actual unsafe
Predicted safe	13	0
Predicted unsafe	9	4

Table 4. Confusion matrix for U-wrap CFRP using Rule 1 ($\omega_V = 0.067$; $\gamma_V = 0.857$).

N = 22	Actual safe	Actual unsafe
Predicted safe	1	1
Predicted unsafe	6	14

The second set of rules was generated with the objective of minimizing the false positives (ω) while keeping the false negatives (γ) less than 0. The summary of the lower and upper bounds for the side-bonded and U-wrapped CFRP is shown in Table 5. A model configured to minimize false negatives generally yields more conservative results, which are ideal to generate V_f values that would render composite systems safe. The corresponding confusion matrices are given in Table 6 and Table 7.

The 2022 World Congress on
The 2022 Structures Congress (Structures22)
 16-19, August, 2022, GECE, Seoul, Korea

Table 5. Boundaries for the parameters under Rule 2.

Parameter	Unit	Side-bonded		U-wrapped	
		X_i^L	X_i^U	X_i^L	X_i^U
f'_c	MPa	22.5	71.4	16.7	39.2
a/d	-	1.22	3.20	1.50	5.00
ρ_s	-	-	0.008	-	0.008
ρ_L	-	0.005	0.040	0.011	0.037
ρ_{FRP}	-	0.0002	0.0267	0.0005	0.0028
d_f	mm	110.0	500.0	153.1	542.9
ε_u	%	7.7	19.2	10.5	20.7

Table 6. Confusion matrix for side-bond CFRP using Rule 2 ($\omega_V = 0.000$; $\gamma_V = 0.455$).

N = 26	Actual safe	Actual unsafe
Predicted safe	12	0
Predicted unsafe	10	4

Table 7. Confusion matrix for U-wrap CFRP using Rule 2 ($\omega_V = 0.333$; $\gamma_V = 0.571$).

N = 22	Actual safe	Actual unsafe
Predicted safe	3	5
Predicted unsafe	4	10

Multiple hyperboxes can also be utilized to explore other decision models, which may yield higher accuracies. This scenario can be executed by changing the predefined number of hyperboxes through the MILP framework. The logical disjunction "OR" is also added in the decision model for every hyperbox created.

Table 8. Boundaries for the parameters under Rule 3.

Group	Parameter	Unit	Side-bonded		U-wrapped	
			X_i^L	X_i^U	X_i^L	X_i^U
Box 1	f'_c	MPa	22.2	71.7	22.4	32.8
	a/d	-	1.19	3.13	1.50	5.02
	ρ_s	-	-	0.008	-	0.008
	ρ_L	-	0.014	0.040	0.017	0.048
	ρ_{FRP}	-	0.0012	0.0118	0.0007	0.0008
	d_f	mm	112.6	500.0	253.1	542.9
	ε_u	%	15.0	19.3	10.5	20.6
Box 2	f'_c	MPa	22.2	70.7	16.4	50.7
	a/d	-	1.22	3.20	3.20	4.98
	ρ_s	-	-	0.008	-	0.008
	ρ_L	-	0.005	0.037	0.010	0.032
	ρ_{FRP}	-	-	0.0267	0.0004	0.0022
	d_f	mm	107.5	500.0	200.0	416.9
	ε_u	%	7.6	17.0	15.0	20.7

*The 2022 World Congress on
The 2022 Structures Congress (Structures22)
16-19, August, 2022, GECE, Seoul, Korea*

A possible disadvantage is the added complexity to the algorithm, which may result in the generation of a slower or unattainable result. Nevertheless, this study adopts a two-hyperbox approach to the two CFRP configurations set to minimize false positives while keeping false negatives less than 0.

Table 9. Confusion matrix for side-bond CFRP using Rule 3 ($\omega_V = 0.000$; $\gamma_V = 0.545$).

N = 26	Actual safe	Actual unsafe
Predicted safe	10	0
Predicted unsafe	12	4

Table 10. Confusion matrix for U-wrap CFRP using Rule 3 ($\omega_V = 0.000$; $\gamma_V = 0.857$).

N = 22	Actual safe	Actual unsafe
Predicted safe	1	0
Predicted unsafe	6	15

The accuracy must be assessed to determine the best-performing models for each configuration. The value for accuracy is given by Eq. (22) and the respective training accuracies for each model are given in Table 11. The results indicate that the best performing models for the two CFRP configurations are Rule 1 (side-bonded) and Rule 3 (U-wrapped) with the highest accuracies at 65.38% and 100.00%, respectively.

$$Accuracy = \frac{True\ Positive + True\ Neative}{Total\ Samples} \quad (22)$$

Table 11. Accuracy yields for the rule-based models.

No. of Hyperboxes	Rule	Configuration	Training Objective	Accuracy, %
One	Rule 1	S-bonded	Minimize γ, $\omega < 0$	65.38
	Rule 1	U-wrapped	Minimize γ , $\omega < 0$	68.18
	Rule 2	S-bonded	Minimize ω , $\gamma < 0$	61.54
	Rule 2	U-wrapped	Minimize ω , $\gamma < 0$	59.09
Two	Rule 3	S-bonded	Minimize ω , $\gamma < 0$	53.85
	Rule 3	U-wrapped	Minimize ω, $\gamma < 0$	100.00

Assessment of the best-performing models was done with 52 retrofitted RC beams. It should be noted that these beams are different from those analyzed by the ML program. The configurations were split into 44% for the s-bonded CFRP and 56% for the U-wrapped CFRP, accounting for 23 and 29 beams, respectively. Table 12 and Table 13 summarize the corresponding performances of the best-performing models of each CFRP configuration. A red cell indicates that a sample is outside the boundaries for the said parameter. The sample must be within limits across all characteristics to be predicted safe (i.e., assigned a model value of 1). The μ is then assessed using

The 2022 World Congress on
The 2022 Structures Congress (Structures22)
 16-19, August, 2022, GECE, Seoul, Korea

$V_{f,theoretical}$ values based on ACI and *fib* 14. A sample is concluded to be accurately predicted if the model prediction matches the respective μ value of the design code.

Table 12. Performances of governing model for side-bonded CFRP vs. design codes.

Ref	Parameters							Model	Design Code		Conclusion	
	f'_c	a/d	ρ_s	ρ_L	ρ_{FRP}	d_f	ϵ_u		ACI	<i>fib</i>	ACI	<i>fib</i>
Ma et al. 2020	37.4	1.88	0.001	0.006	0.0003	300.0	21.3	unsafe	unsafe	unsafe	correct	correct
	37.4	1.88	0.001	0.006	0.0006	300.0	21.3	unsafe	unsafe	unsafe	correct	correct
	32.8	2.84	0.000	0.031	0.0007	300.0	14.8	unsafe	safe	safe	wrong	wrong
Beber and Campos	32.8	2.84	0.000	0.031	0.0007	300.0	14.8	unsafe	safe	safe	wrong	wrong
	32.8	2.84	0.000	0.031	0.0015	300.0	14.8	safe	safe	safe	correct	correct
Filho 2005	32.8	2.84	0.000	0.031	0.0015	300.0	14.8	safe	safe	safe	correct	correct
	32.8	2.84	0.000	0.031	0.0093	300.0	12.2	safe	unsafe	unsafe	wrong	wrong
	32.8	2.84	0.000	0.031	0.0066	300.0	12.2	safe	unsafe	unsafe	wrong	wrong
Salama et al. 2019	47.2	2.16	0.010	0.006	0.0136	100.0	21.0	unsafe	safe	unsafe	wrong	correct
	47.2	2.16	0.010	0.006	0.0272	100.0	21.0	unsafe	safe	unsafe	wrong	correct
	47.2	2.16	0.010	0.006	0.0136	150.0	21.0	unsafe	unsafe	unsafe	correct	correct
	47.2	2.16	0.010	0.006	0.0272	150.0	21.0	unsafe	unsafe	unsafe	correct	correct
	47.2	2.16	0.010	0.006	0.0272	50.0	21.0	unsafe	safe	unsafe	wrong	correct
Allam and Ebeido 2003	40.0	2.57	0.003	0.029	0.0011	200.0	15.2	safe	safe	safe	correct	correct
	40.0	2.57	0.003	0.029	0.0011	200.0	15.2	safe	safe	safe	correct	correct
	40.0	2.57	0.003	0.029	0.0022	200.0	15.2	safe	safe	safe	correct	correct
	40.0	2.57	0.003	0.029	0.0022	200.0	15.2	safe	safe	safe	correct	correct
Allam and Ebeido 2003	40.0	2.57	0.003	0.029	0.0011	200.0	15.2	safe	safe	safe	correct	correct
	40.0	1.71	0.003	0.029	0.0011	200.0	15.2	safe	safe	safe	correct	correct
	40.0	1.71	0.003	0.029	0.0022	200.0	15.2	safe	safe	safe	correct	correct

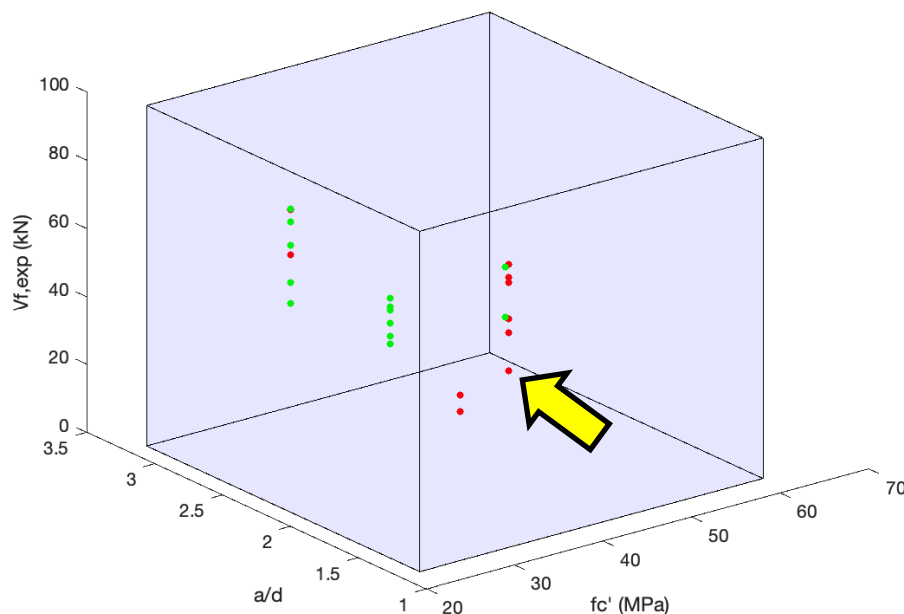
Table 13. Performances of governing model for U-wrapped CFRP vs. design codes.

Ref	Parameters							Model	Design Code		Conclusion	
	f'_c	a/d	ρ_s	ρ_L	ρ_{FRP}	d_f	ϵ_u		ACI	<i>fib</i>	ACI	<i>fib</i>
Ma et al. 2020	37.4	1.88	0.001	0.006	0.0003	300.0	21.3	unsafe	unsafe	unsafe	correct	correct
	37.4	1.88	0.001	0.006	0.0006	300.0	21.3	unsafe	unsafe	unsafe	correct	correct
	32.8	2.84	0.000	0.031	0.0007	300.0	14.8	safe	safe	safe	correct	correct
	32.8	2.84	0.000	0.031	0.0007	300.0	14.8	safe	safe	safe	correct	correct
Beber and Campos Filho 2005	32.8	2.84	0.000	0.031	0.0007	300.0	14.8	safe	safe	safe	correct	correct
	32.8	2.84	0.000	0.031	0.0007	300.0	14.8	safe	safe	safe	correct	correct
	32.8	2.84	0.000	0.031	0.0005	300.0	14.8	unsafe	safe	safe	wrong	wrong
Alzate et al. 2013	32.8	2.84	0.000	0.031	0.0015	300.0	14.8	unsafe	safe	safe	wrong	wrong
	32.8	2.84	0.000	0.031	0.0015	300.0	14.8	unsafe	unsafe	safe	correct	correct
	24.5	3.49	0.001	0.021	0.0023	420.0	16.7	unsafe	unsafe	unsafe	correct	correct
	30.7	3.49	0.001	0.021	0.0014	420.0	16.7	unsafe	unsafe	unsafe	correct	correct
	30.2	3.49	0.001	0.021	0.0013	420.0	15.8	unsafe	unsafe	unsafe	correct	correct
	30.2	3.49	0.001	0.021	0.0013	420.0	15.8	unsafe	unsafe	unsafe	correct	correct
	20.5	3.49	0.001	0.021	0.0008	420.0	15.8	unsafe	unsafe	unsafe	correct	correct
	30.7	3.49	0.001	0.021	0.0008	420.0	15.8	safe	unsafe	unsafe	wrong	wrong
	27.4	2.50	0.000	0.017	0.0008	340.0	16.5	unsafe	unsafe	unsafe	correct	correct
	27.4	2.50	0.000	0.017	0.0008	340.0	16.5	unsafe	safe	safe	wrong	wrong
Jayapra-Kash et al 2008	27.4	2.50	0.000	0.011	0.0006	340.0	16.5	unsafe	unsafe	unsafe	correct	correct
	16.7	4.00	0.000	0.017	0.0008	340.0	16.5	safe	safe	safe	correct	correct
	16.7	4.00	0.000	0.017	0.0008	340.0	16.5	safe	safe	safe	correct	correct
	16.7	4.00	0.000	0.011	0.0008	340.0	16.5	safe	unsafe	unsafe	wrong	wrong
	16.7	4.00	0.000	0.011	0.0008	340.0	16.5	safe	unsafe	unsafe	wrong	wrong
	16.7	4.00	0.000	0.011	0.0008	340.0	16.5	safe	unsafe	unsafe	wrong	wrong
Norris et al. 1997	36.5	2.57	0.002	0.018	0.0315	203.0	11.4	unsafe	unsafe	unsafe	correct	correct
	36.5	2.57	0.002	0.018	0.0315	203.0	11.4	unsafe	unsafe	unsafe	correct	correct
	36.5	2.57	0.002	0.018	0.0315	203.0	11.8	unsafe	unsafe	unsafe	correct	correct
	36.5	2.57	0.002	0.018	0.0236	203.0	8.7	unsafe	unsafe	unsafe	correct	correct

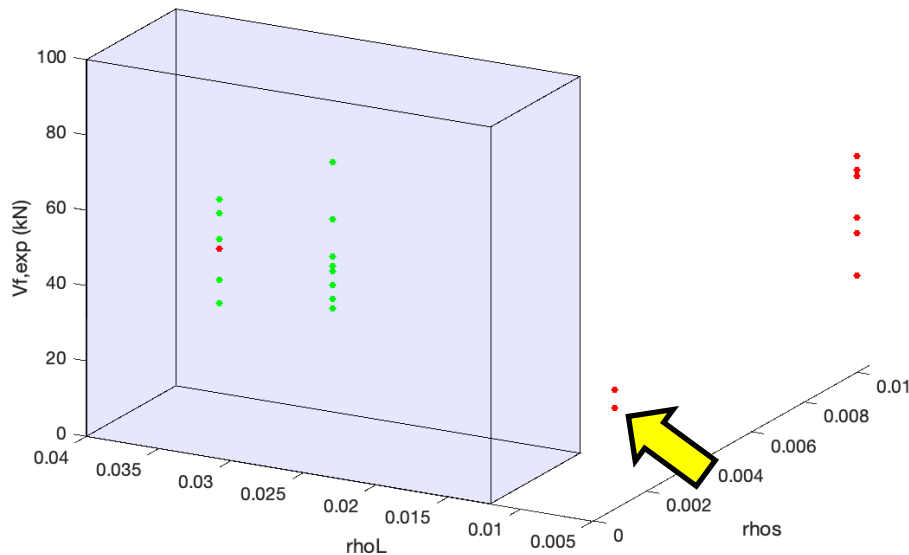
The 2022 World Congress on
The 2022 Structures Congress (Structures22)
16-19, August, 2022, GECE, Seoul, Korea

A 3D visualization of the hyperboxes on two parameter axes can be done to assess samples like those found in Table 12 and Table 13. The blue boxes in Figure 1 represent the hyperboxes following the dimensions of the governing models. For example, the governing model for the side-bonded CFRP is Rule 1 (Table 2), and the concrete compressive strength follows the range $[22.2 \leq f'_c \leq 61.0]$. When the sample is inside the hyperbox concerning all the parameters, it is predicted safe. Conversely, when a sample is outside of the the hyperbox for at least one parameter, then it is predicted unsafe. Samples predicted to be safe are marked green, while those indicated as unsafe are marked red. The following example shows a visualiazation of a retrofitted RC beam predicted unsafe using the sample from [Ma et al \(2020\)](#) (first sample indicated in Table 12) shown in Figure 1. The sample is indicated by the yellow arrows.

Visualizations in ML assessment, though uncommon, play an important role especially in research and structural engineering. A primary function of 3D visualization is to provide decision-makers (e.g., engineers) a graphical view of any occurring trends concerning the hyperbox dimensions. This functionality may provide new insights on the influential parameters determined or the rule-based models generated (e.g., many samples fail the overall criteria due to certain parameter/s).



(a) point is within boundary of f'_c and a/d



(b) point is within boundary of ρ_S but not ρ_L

Figure 1. 3D visualization of the side bonded CFRP beam sample (Ma et al) predicted as unsafe by the model.

The rule-based models produced in this study gave satisfactory results concerning similar studies reviewed (Abuodeh et al 2020; Zhou et al 2020; Kar et al 2021). A summary of the performances is given in Figure 2. The results of the governing hyperbox model for the S-bonded CFRP yielded 18 of 23 (or 78%) and 15 of 23 (or 65%) correct predictions using the *fib 14* and ACI, respectively. Meanwhile, the results of the governing hyperbox model for the U-wrapped CFRP yielded 21 of 29 (or 72%) and 22 of 29 (or 76%) correct predictions using the *fib 14* and ACI, respectively.

The discrepancies between the figure above and the results from the validation phase illustrate several limitations of the MILP-based hyperbox classification modeling approach. One limitation is being unable to yield the same degree of accuracy consistently. This limitation can partially be attributed to the limited samples that the MILP can process to determine a global optimum. Another limitation is the non-consideration of external factors in constructing this database. Only parameters explicitly given in the references (or required only minimal calculations and assumptions) were further processed to enhance the likelihood of producing an accurate model.

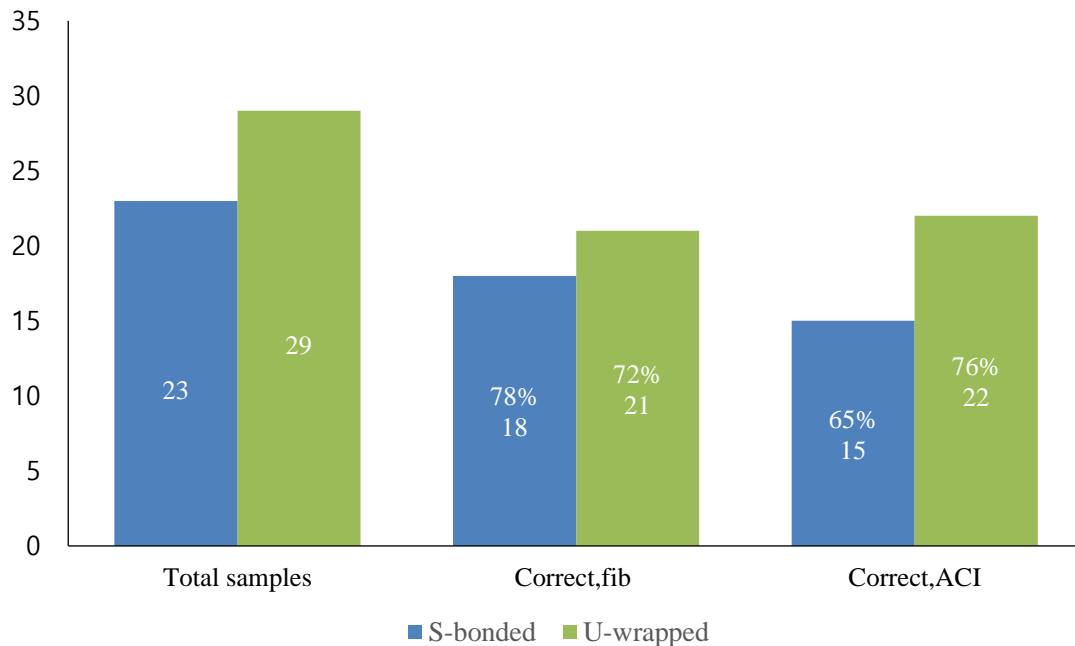


Figure 2. Performance summary of governing rule-based models.

5. CONCLUSIONS AND RECOMMENDATIONS

The produced rule-based equations showcase an ML application with hyperboxes using a novel MILP approach. The work presented serves as an example of solving problems requiring binary decisions for critical but ambiguous scenarios. False positive (or Type 1) occurrences are considered the critical errors in this scenario. The best-performing models determine if the composite CFRP-RC systems are safe based on the shear contribution (V_f) of the EB CFRP. This study analyzed only side-bonded and U-wrapped CFRP on simply supported beams. The processed data from the combined samples reveal that there are seven influential parameters determining V_f of the EB CFRP. The governing models yielded accuracies of 65.38% and 100.0% for the side-bonded and U-wrapped CFRP, respectively, and mitigated the occurrence of false positives during the validation phase. The governing models yielded accurate predictions of 78% (S-bonded) and 72% (U-wrapped) with *fib 14* and 65% (S-bonded) and 76% (U-wrapped) with ACI. The rule-based hyperbox models generated provided a feature of minimizing misclassification errors during their creation phase, translating to minimal prediction errors in actual applications. Therefore, a marked advantage for the hyperbox models is demonstrated over the capabilities of existing design codes. Overall, the models can serve as decision guidelines amidst the uncertainties in complex behaviors like shear mechanics.

Nevertheless, improvements can be made by future research to improve the accuracy yields of the best-performing rule-based models. One possibility is to try different frameworks aside from MILP for classifying samples. Another recommendation

*The 2022 World Congress on
The 2022 Structures Congress (Structures22)
16-19, August, 2022, GECE, Seoul, Korea*

is to derive closed-form solutions to analyze the effects of the parameters in determining the sufficiency of CFRP shear contribution.

REFERENCES

- Abuodeh, O. R., Abdalla, J. A., & Hawileh, R. A. (2020). Prediction of shear strength and behavior of RC beams strengthened with externally bonded FRP sheets using machine learning techniques. *Composite Structures*, 234, 111698.
- ACI Committee 440, & Busel, J. P. (2008). Specification for carbon and glass fiber-reinforced polymer bar materials for concrete reinforcement. American Concrete Institute.
- Adhikari, S. (2009). Mechanical properties and flexural applications of basalt fiber reinforced polymer (BFRP) bars (Doctoral dissertation, University of Akron).
- Akroush, N., Almahallawi, T., Seif, M., & Sayed-Ahmed, E. Y. (2017). CFRP shear strengthening of reinforced concrete beams in zones of combined shear and normal stresses. *Composite Structures*, 162, 47-53.
- Al-Mahaidi, R., & Kalfat, R. (2018). Rehabilitation of concrete structures with fiber-reinforced polymer. Butterworth-Heinemann.
- Al-Saawani, M. A., El-Sayed, A. K., & Al-Negheimish, A. I. (2020). Effect of shear-span/depth ratio on debonding failures of FRP-strengthened RC beams. *Journal of Building Engineering*, 32, 101771.
- Alhroob, E., Mohammed, M. F., Lim, C. P., & Tao, H. (2019). A critical review on selected fuzzy min-max neural networks and their significance and challenges in pattern classification. *IEEE access*, 7, 56129-56146.
- Amran, Y. M., Alyousef, R., Rashid, R. S., Alabduljabbar, H., & Hung, C. C. (2018, November). Properties and applications of FRP in strengthening RC structures: A review. In *Structures* (Vol. 16, pp. 208-238). Elsevier.
- Aviso, K. B., Demeterio III, F. P. A., Janairo, J. I. B., Lucas, R. I. G., Promentilla, M. A. B., Tan, R. R., & Yu, D. E. C. (2021). What University Attributes Predict for Graduate Employability?. *Cleaner Engineering and Technology*, 100069.
- Azad, C., Mehta, A. K., & Jha, V. K. (2018, July). Improved data classification using fuzzy euclidean hyperbox classifier. In 2018 International Conference on Smart Computing and Electronic Enterprise (ICSCEE) (pp. 1-6). IEEE.
- Belarbi, A., & Acun, B. (2013). FRP systems in shear strengthening of reinforced concrete structures. *Procedia Engineering*, 57, 2-8.
- Breña, S. F., Bramblett, R. M., Benouaich, M. A., Wood, S. L., & Kreger, M. E. (2001). Use of carbon fiber reinforced polymer composites to increase the flexural capacity of reinforced concrete beams (No. Research Report 1776-1). University of Texas at Austin.
- Ceroni, F., Cosenza, E., Gaetano, M., & Pecce, M. (2006). Durability issues of FRP rebars in reinforced concrete members. *Cement and concrete composites*, 28(10), 857-868.
- Chaabene, W. B., Flah, M., & Nehdi, M. L. (2020). Machine learning prediction of mechanical properties of concrete: Critical review. *Construction and Building Materials*, 260, 119889.
- Chaallal, O., Nollet, M. J., & Perraton, D. (1998). Strengthening of reinforced concrete beams with externally bonded fiber-reinforced-plastic plates: design guidelines for shear and flexure. *Canadian Journal of Civil Engineering*, 25(4), 692-704.
- Chandrakar, J., & Singh, A. K. (2017). Study of Various Local and Global Seismic Retrofitting Strategies—A review. *Int. J. Eng. Res. Technol*, 6, 824-831.
- Chen, G. M., Li, S. W., Fernando, D., Liu, P. C., & Chen, J. F. (2017). Full-range FRP failure behaviour in RC beams shear-strengthened with FRP wraps. *International Journal of Solids and Structures*, 125, 1-21.
- Chen, G. M., Teng, J. G., & Chen, J. F. (2013). Shear strength model for FRP-strengthened RC beams with adverse FRP-steel interaction. *Journal of Composites for Construction*, 17(1), 50-66.

*The 2022 World Congress on
The 2022 Structures Congress (Structures22)
16-19, August, 2022, GECE, Seoul, Korea*

- Chen, J. F., & Teng, J. G. (2003). Shear capacity of fiber-reinforced polymer-strengthened reinforced concrete beams: Fiber reinforced polymer rupture. *Journal of Structural Engineering*, 129(5), 615-625.
- Colotti, V. (2016). Mechanical shear strength model for reinforced concrete beams strengthened with FRP materials. *Construction and Building Materials*, 124, 855-865.
- Das, S. (2011). Life cycle assessment of carbon fiber-reinforced polymer composites. *The International Journal of Life Cycle Assessment*, 16(3), 268-282.
- El-Maaddawy, T., & Chekfeh, Y. (2012). Retrofitting of severely shear-damaged concrete t-beams using externally bonded composites and mechanical end anchorage. *Journal of Composites for Construction*, 16(6), 693-704.
- Godat, A., Labossière, P., & Neale, K. W. (2012). Numerical investigation of the parameters influencing the behaviour of FRP shear-strengthened beams. *Construction and Building Materials*, 32, 90-98.
- Hanoon, A. N., Jaafar, M. S., Hejazi, F., & Aziz, F. N. A. (2017). Strut-and-tie model for externally bonded CFRP-strengthened reinforced concrete deep beams based on particle swarm optimization algorithm: CFRP debonding and rupture. *Construction and Building Materials*, 147, 428-447.
- Huang, Z., Tu, Y., Meng, S., Sabau, C., Popescu, C., & Sas, G. (2019). Experimental study on shear deformation of reinforced concrete beams using digital image correlation. *Engineering Structures*, 181, 670-698.
- Huo, J., Li, Z., Zhao, L., Liu, J., & Xiao, Y. (2018). Dynamic behavior of carbon fiber-reinforced polymer-strengthened reinforced concrete beams without stirrups under impact loading. *ACI Structural Journal*, 115(3), 775-787.
- John, K., & Naidu, S. V. (2004). Tensile properties of unsaturated polyester-based sisal fiber-glass fiber hybrid composites. *Journal of Reinforced Plastics and Composites*, 23(17), 1815-1819.
- Kar, S., Pandit, A. R., & Biswal, K. C. (2021). A neuro-fuzzy approach to estimate the shear contribution of externally bonded FRP composites. *Asian Journal of Civil Engineering*, 22(2), 351-367.
- Karzad, A. S., Leblouba, M., Al Toubat, S., & Maalej, M. (2019). Repair and strengthening of shear-deficient reinforced concrete beams using Carbon Fiber Reinforced Polymer. *Composite Structures*, 223, 110963.
- Khalifa, A., Gold, W. J., Nanni, A., & MI, A. A. (1998). Contribution of externally bonded FRP to shear capacity of RC flexural members. *Journal of composites for construction*, 2(4), 195-202.
- Khuat, T. T., Ruta, D., & Gabrys, B. (2021). Hyperbox-based machine learning algorithms: a comprehensive survey. *Soft Computing*, 25(2), 1325-1363.
- Landesmann, A., Seruti, C. A., & Batista, E. D. M. (2015). Mechanical properties of glass fiber reinforced polymers members for structural applications. *Materials Research*, 18(6), 1372-1383.
- Lavorato, D., Nuti, C., & Santini, S. (2018). Experimental investigation of the shear strength of RC beams extracted from an old structure and strengthened by carbon FRP U-strips. *Applied Sciences*, 8(7), 1182.
- Lee, D. H., Kim, K. S., Han, S. J., Zhang, D., & Kim, J. (2018). Dual potential capacity model for reinforced concrete short and deep beams subjected to shear. *Structural Concrete*, 19(1), 76-85.
- Lee, J. Y., Hwang, H. B., & Doh, J. H. (2012). Effective strain of RC beams strengthened in shear with FRP. *Composites Part B: Engineering*, 43(2), 754-765.
- Li, W., & Leung, C. K. (2016). Shear span-depth ratio effect on behavior of RC beam shear strengthened with full-wrapping FRP strip. *Journal of Composites for Construction*, 20(3), 04015067.
- Lütjering, G., & Williams, J. C. (2007). *Titanium*. Springer Science & Business Media.
- Ma, S., Muhamad Bunnori, N., & Choong, K. K. (2020). Experimental study on shear strengthening of reinforced concrete box beam by CFRP. *Iranian Journal of Science and Technology, Transactions of Civil Engineering*, 44(4), 1075-1085.
- Mansouri, I., Kisi, O., Sadeghian, P., Lee, C. H., & Hu, J. W. (2017). Prediction of ultimate strain and strength of FRP-confined concrete cylinders using soft computing methods. *Applied Sciences*, 7(8), 751.

*The 2022 World Congress on
The 2022 Structures Congress (Structures22)
16-19, August, 2022, GECE, Seoul, Korea*

- Meier, U. (1991). Strengthening of structures with CFRP. In *Advanced Composite Materials in Civil Engineering Structures*, Proc. Specialty Conf. Las Vegas, NV (pp. 224-232). ASCE.
- Mhanna, H. H., Hawileh, R. A., & Abdalla, J. A. (2019). Shear strengthening of reinforced concrete beams using CFRP wraps. *Procedia Structural Integrity*, 17, 214-221.
- Miller, T. C., Chajes, M. J., Mertz, D. R., & Hastings, J. N. (2001). Strengthening of a steel bridge girder using CFRP plates. *Journal of bridge engineering*, 6(6), 514-522.
- Mostofinejad, D., & Kashani, A. T. (2013). Experimental study on effect of EBR and EBROG methods on debonding of FRP sheets used for shear strengthening of RC beams. *Composites Part B: Engineering*, 45(1), 1704-1713.
- Naderpour, H., & Alavi, S. A. (2017). A proposed model to estimate shear contribution of FRP in strengthened RC beams in terms of Adaptive Neuro-Fuzzy Inference System. *Composite Structures*, 170, 215-227.
- Naser, M. Z., Hawileh, R. A., & Abdalla, J. A. (2019). Fiber-reinforced polymer composites in strengthening reinforced concrete structures: A critical review. *Engineering Structures*, 198, 109542.
- Oller, E., Kotynia, R., & Marí, A. (2021). Assessment of the existing models to evaluate the shear strength contribution of externally bonded FRP shear reinforcements. *Composite Structures*, 266, 113641.
- Ongpeng J., Lecciones I.N., Garduque J.A., Buera D.J. (2020). Ultimate Confined Compressive Strength of Carbon Fiber-Reinforced Circular and Rectangular Concrete Column. In: Alfred R., Lim Y., Haviluddin H., On C. (eds) *Computational Science and Technology. Lecture Notes in Electrical Engineering*, vol 603. Springer, Singapore. https://doi.org/10.1007/978-981-15-0058-9_34
- Pampanin, S., Bolognini, D., & Pavese, A. (2007). Performance-based seismic retrofit strategy for existing reinforced concrete frame systems using fiber-reinforced polymer composites. *Journal of Composites for Construction*, 11(2), 211-226.
- Peng, L., & Stewart, M. G. (2014). Spatial time-dependent reliability analysis of corrosion damage to RC structures with climate change. *Magazine of Concrete Research*, 66(22), 1154-1169.
- Pohoryles, D. A., Melo, J., Rossetto, T., Fabian, M., McCague, C., Stavrianaki, K., ... & Sargeant, B. (2017). Use of DIC and AE for monitoring effective strain and debonding in FRP and FRCM-retrofitted RC beams. *Journal of Composites for Construction*, 21(1), 04016057.
- Qureshi, H. J., & Saleem, M. U. (2018). Flexural and shear strain characteristics of carbon fiber reinforced polymer composite adhered to a concrete surface. *Materials*, 11(12), 2596.
- Salama, A. S. D., Hawileh, R. A., & Abdalla, J. A. (2019). Performance of externally strengthened RC beams with side-bonded CFRP sheets. *Composite Structures*, 212, 281-290.
- Saleem, M. U., Qureshi, H. J., Amin, M. N., Khan, K., & Khurshid, H. (2019). Cracking behavior of RC beams strengthened with different amounts and layouts of CFRP. *Applied Sciences*, 9(5), 1017.
- Sarasini, F., Tirillò, J., Ferrante, L., Valente, M., Valente, T., Lampani, L., ... & Sorrentino, L. (2014). Drop-weight impact behaviour of woven hybrid basalt-carbon/epoxy composites. *Composites Part B: Engineering*, 59, 204-220.
- Schmidt, M., Schmidt, P., Wanka, S., & Classen, M. (2021). Shear Response of Members without Shear Reinforcement—Experiments and Analysis Using Shear Crack Propagation Theory (SCPT). *Applied Sciences*, 11(7), 3078.
- Siddika, A., Al Mamun, M. A., Ferdous, W., & Alyousef, R. (2020). Performances, challenges and opportunities in strengthening reinforced concrete structures by using FRPs—A state-of-the-art review. *Engineering Failure Analysis*, 104480.
- Simpson, P. K. (1992). Fuzzy min—max neural networks—Part 1: Classification. *IEEE Trans. on Neural Networks*, 3(5), 776-786.
- Singh, S. B. (2013). Shear response and design of RC beams strengthened using CFRP laminates. *International Journal of Advanced Structural Engineering*, 5(1), 1-16.

*The 2022 World Congress on
The 2022 Structures Congress (Structures22)
16-19, August, 2022, GECE, Seoul, Korea*

- Song, Y. Y., & Ying, L. U. (2015). Decision tree methods: applications for classification and prediction. *Shanghai archives of psychiatry*, 27(2), 130.
- Tan, R. R., Aviso, K. B., Janairo, J. I. B., & Promentilla, M. A. B. (2020). A hyperbox classifier model for identifying secure carbon dioxide reservoirs. *Journal of Cleaner Production*, 272, 122181.
- Triantafillou, T. C. (1998). Shear strengthening of reinforced concrete beams using epoxy-bonded FRP composites. *ACI structural journal*, 95, 107-115.
- Xu, G., & Papageorgiou, L. G. (2009). A mixed integer optimisation model for data classification. *Computers & Industrial Engineering*, 56(4), 1205-1215.
- Zadeh, L. A. (1965). Fuzzy sets. *Information and control*, 8(3), 338-353.
- Zhou, Y., Zhang, J., Li, W., Hu, B., & Huang, X. (2020). Reliability-based design analysis of FRP shear strengthened reinforced concrete beams considering different FRP configurations. *Composite Structures*, 237, 111957.